Available online at www.sciencedirect.com
ScienceDirect
Journal of Sound and Vibration 306 (2007) 818–834
JOURNAL OF SOUND AND VIBRATION
www.elsevier.com/locate/jsvi

Vibration analysis of 3-D composite beam elements including warping and shear deformation effects

E.J. Sapountzakis*, V.G. Mokos

School of Civil Engineering, National Technical University, Zografou Campus, GR-157 80 Athens, Greece

Received 4 January 2007; received in revised form 27 June 2007; accepted 27 June 2007

Abstract

In this paper, the dynamic analysis of 3-D composite beam elements restrained at their edges by the most general boundary conditions and subjected in arbitrarily distributed dynamic loading is presented. For the solution of the problem at hand, a boundary element method is developed for the construction of the 14×14 stiffness matrix and the nodal load vector of a member of an arbitrarily shaped composite cross section, taking into account both torsional warping and shear deformation effects, which together with the corresponding mass and damping matrices lead to the formulation of the equation of motion. To account for shear deformations, the concept of shear deformation coefficients is used, defining these factors using a strain energy approach. Eight boundary value problems with respect to the variable along the bar angle of twist, to the primary warping function, to a fictitious function, to the beam transverse and longitudinal displacements and to two stress functions are formulated and solved employing a pure BEM approach. Both free and forced vibrations are considered, taking also into account effects of transverse, longitudinal, rotatory, torsional and warping inertia and damping resistance. Numerical examples are presented to illustrate the method and demonstrate its efficiency and accuracy.

1. Introduction

One of the problems often encountered in engineering practice is the dynamic analysis of rectilinear or curved composite members of structures, subjected to vibratory transverse, longitudinal or twisting loading. The dynamic forces acting on a structure may result from one or more of different causes, such as rotating machinery, wind, symmetric and asymmetric traffic loading, blast loads or earthquake forces. Composite structural elements, consisting of a relatively weak matrix reinforced by stronger inclusions or of different materials in contact, are of increasing technological importance in engineering. Steel beams or columns totally encased in concrete are most common examples, while construction using steel beams as stiffeners of concrete plates is a quick, familiar and economical method for long bridge decks or for long span slabs. The extensive use of the aforementioned structural elements necessitates a rigorous dynamic analysis. However, accurate dynamic analysis in engineering practice is difficult to be achieved for two reasons.

*Corresponding author. Tel.: +30 210 7721718; fax: +30 210 7721720.
E-mail addresses: cvsapoun@central.ntua.gr (E.J. Sapountzakis), vgmokos@central.ntua.gr (V.G. Mokos).

0022-460X/$ - see front matter © 2007 Elsevier Ltd. All rights reserved.
doi:10.1016/j.jsv.2007.06.021

According to the first reason, the most general commercial programs (with very few exceptions [1,2]) consider six degrees of freedom at each node of a member of a space frame, ignoring in this way the torsional warping effects due to the corresponding restraint at the ends of the member [3]. If the aforementioned structures are analyzed or designed for torsion, considering only the effect of Saint Venant torsion resistance, the analysis may underestimate the torsion in the members and the design may be unconservative. Several researchers tried to overcome this inaccuracy by developing a 14×14 member stiffness matrix including torsional warping degrees of freedom at the ends of a member with open thin-walled homogeneous cross section and assuming simple [4–7] or more complicated torsional boundary conditions [8,9]. It is worth noting here that the solutions obtained from commercial finite-element packages, which have the possibility of considering seven degrees of freedom at each node including warping degree of freedom (dof) [1,2] are not exact because stiffness matrices are generated with linear and quadratic shape functions.

According to the second reason, the commercial programs that take into account shear deformations ignore the effect of Poisson's ratio as well as the coupled boundary conditions at the interfaces between different materials, facing the composite cross section as one consisting of internal regions of different materials. Though these deformations are quite small in most civil engineering applications, they may be dominant in some situations, where bending moments are small compared to shear forces acting on the member. This is normally true in short span beams or in structural systems such as curved box girder bridges.

Moreover, in the case of composite beams of thin-walled or laminated cross sections the aforementioned problem can also be solved using the 'refined models' [10–13]. However, these models do not satisfy the continuity conditions of transverse shear stress at layer interfaces and assume that the transverse shear stress along the thickness coordinate remains constant, leading to the fact that kinematic or static assumptions cannot be always valid.

In this paper, the dynamic analysis of 3-D composite beam elements subjected in dynamic twisting, bending, transverse or longitudinal arbitrary loading is presented. Their arbitrarily shaped composite cross section consists of materials in contact each of which can surround a finite number of inclusions, while their ends are supported by the most general linear torsional, transverse or longitudinal boundary conditions. All the cross section materials is assumed to have the same Poisson's ratio. The solution of the aforementioned problem is achieved by employing the boundary element method for the construction of the 14×14 stiffness matrix and the nodal load vector, taking into account both torsional warping and shear deformation effects, which together with the corresponding mass and damping matrices lead to the formulation of the equation of motion. The construction of the aforementioned stiffness matrix and nodal load vector is achieved by solving directly the governing differential equations using the BEM, contrary to previous formulations employing the FEM, where the accuracy depends on the effective selection of the shape functions. To account for shear deformations, the concept of shear deformation coefficients is used. In this investigation the definition of these factors is accomplished using a strain energy approach [14,15], instead of Timoshenko's [16] and Cowper's [17] definitions, for which several authors [18,19] have pointed out that one obtains unsatisfactory results or definitions given by other researchers [20,21], for which these factors take negative values. Eight boundary value problems with respect to the variable along the bar angle of twist, to the primary warping function, to a fictitious function, to the beam transverse and longitudinal displacements and to two stress functions are formulated and solved employing a pure BEM [22] approach, that is only boundary discretization is used. It is worth noting here that the coupled boundary conditions at the interfaces between different materials for the formulation of the primary warping function, the fictitious function and the two stress functions are taken into account. Both free and forced transverse, longitudinal or torsional vibrations are considered, taking also into account effects of transverse, longitudinal, rotatory, torsional and warping inertia and damping resistance. The proposed method can be efficiently applied to homogeneous and composite beams of thin-walled cross section and to laminated composite beams, without the aforementioned restrictions of the 'refined models'. Numerical examples are presented to illustrate the method and demonstrate its efficiency and accuracy. The influence of the torsional warping effect especially in composite members of open form cross section is analyzed through examples demonstrating the importance of the inclusion of the torsional warping degrees of freedom in the dynamic analysis of a space frame. Moreover, the discrepancy in the dynamic analysis of a member of a spatial structure arising from the ignorance of the shear deformation effect necessitates the inclusion of this additional effect, especially in thick-walled cross section members.

2. Statement of the problem

Consider a prismatic 3-D beam element of length l with an arbitrarily shaped composite cross section consisting of materials in contact, each of which can surround a finite number of inclusions, with modulus of elasticity E_j, shear modulus G_j and mass density ρ_j, occupying the regions Ω_j $(j = 1, 2, \ldots, K)$ of the $\bar{y}$, $\bar{z}$ plane (Fig. 1). The materials of these regions are assumed homogeneous, isotropic and linearly elastic. Let also the boundaries of the nonintersecting regions Ω_j be denoted by Γ_j $(j = 1, 2, \ldots, K)$. These boundary curves are piecewise smooth, i.e. they may have a finite number of corners. Without loss of generality, it may be assumed that $C\tilde{y}\tilde{z}$ and Myz are the principal systems of axes through the cross section's centroid and shear center, respectively.

In order to include the torsional warping behavior in the study of the aforementioned element in each node at the element ends a seventh dof is added to the well-known six dofs of the classical 3-D frame element, which is used in the direct stiffness method. The additional dof is the first derivative of the angle of twist $\theta'_x = \mathrm{d}\theta_x/\mathrm{d}x$ denoting the rate of change of the angle of twist $\theta_x = \theta_x(x, t)$. Thus, the nodal displacement vector in the local coordinate system, as shown in Fig. 1, can be written as

$$\mathbf{D}^{\mathrm{T}} = \left\{ u_{\tilde{x}j} \quad u_{\tilde{y}j} \quad u_{\tilde{z}j} \quad \theta_{xj} \quad \theta_{\tilde{y}j} \quad \theta_{\tilde{z}j} \quad \theta'_{xj} \quad u_{\tilde{x}k} \quad u_{\tilde{y}k} \quad u_{\tilde{z}k} \quad \theta_{xk} \quad \theta_{\tilde{y}k} \quad \theta_{\tilde{z}k} \quad \theta'_{xk} \right\} \tag{1}$$

and the respective nodal load vector as

$$\mathbf{P}^{\mathrm{T}} = \left\{ N_j \quad Q_{yj} \quad Q_{zj} \quad M_{xj} \quad M_{\tilde{y}j} \quad M_{\tilde{z}j} \quad M_{wj} \quad N_k \quad Q_{yk} \quad Q_{zk} \quad M_{xk} \quad M_{\tilde{y}k} \quad M_{\tilde{z}k} \quad M_{wk} \right\}. \tag{2}$$

The nodal displacement and load vectors given in Eqs. (1) and (2) are related with the 14×14 local stiffness matrix of the spatial beam element written as

$$\mathbf{k} = \left[\begin{array}{cccccc|c|cccccc|c}
k_{11} & 0 & 0 & 0 & 0 & 0 & 0 & k_{18} & 0 & 0 & 0 & 0 & 0 & 0 \\
0 & k_{22} & 0 & 0 & 0 & k_{26} & 0 & 0 & k_{29} & 0 & 0 & 0 & k_{2,13} & 0 \\
0 & 0 & k_{33} & 0 & k_{35} & 0 & 0 & 0 & 0 & k_{3,10} & 0 & k_{3,12} & 0 & 0 \\
0 & 0 & 0 & \boxed{k_{T1}} & 0 & 0 & \boxed{k_{T2}} & 0 & 0 & 0 & \boxed{-k_{T1}} & 0 & 0 & \boxed{k_{T5}} \\
0 & 0 & k_{53} & 0 & k_{55} & 0 & 0 & 0 & 0 & k_{5,10} & 0 & k_{5,12} & 0 & 0 \\
0 & k_{62} & 0 & 0 & 0 & k_{66} & 0 & 0 & k_{69} & 0 & 0 & 0 & k_{6,13} & 0 \\
\hline
0 & 0 & 0 & \boxed{k_{T2}} & 0 & 0 & \boxed{k_{T3}} & 0 & 0 & 0 & \boxed{-k_{T2}} & 0 & 0 & \boxed{k_{T4}} \\
\hline
k_{81} & 0 & 0 & 0 & 0 & 0 & 0 & k_{88} & 0 & 0 & 0 & 0 & 0 & 0 \\
0 & k_{92} & 0 & 0 & 0 & k_{96} & 0 & 0 & k_{99} & 0 & 0 & 0 & k_{9,13} & 0 \\
0 & 0 & k_{10,3} & 0 & k_{10,5} & 0 & 0 & 0 & 0 & k_{10,10} & 0 & k_{10,12} & 0 & 0 \\
0 & 0 & 0 & \boxed{-k_{T1}} & 0 & 0 & \boxed{-k_{T2}} & 0 & 0 & 0 & \boxed{k_{T5}} & 0 & 0 & \boxed{-k_{T5}} \\
0 & 0 & k_{12,3} & 0 & k_{12,5} & 0 & 0 & 0 & 0 & k_{12,10} & 0 & k_{12,12} & 0 & 0 \\
0 & k_{13,2} & 0 & 0 & 0 & k_{13,6} & 0 & 0 & k_{13,9} & 0 & 0 & 0 & k_{13,13} & 0 \\
\hline
0 & 0 & 0 & \boxed{k_{T5}} & 0 & 0 & \boxed{k_{T4}} & 0 & 0 & 0 & \boxed{-k_{T5}} & 0 & 0 & \boxed{k_{T6}}
\end{array}\right], \tag{3}$$

where the k^i_{Tn} $(n = 1, 2, 3, 4, 5, 6)$ stiffness coefficients contain the torsional warping effects, while the k^i_{lm} stiffness coefficients $(l, m = 2, 3, 5, 6, 9, 10, 12, 13)$ contain the shear deformation effects following the so-called Timoshenko beam theory. The evaluation of the coefficients of the 14×14 stiffness matrix of Eq. (3), of the nodal load vector of Eq. (2) and of the mass and damping matrices presumes the solution of four initial boundary value problems with respect to the variable along the bar angle of twist and to the beam transverse and longitudinal displacements that are analyzed in the following.

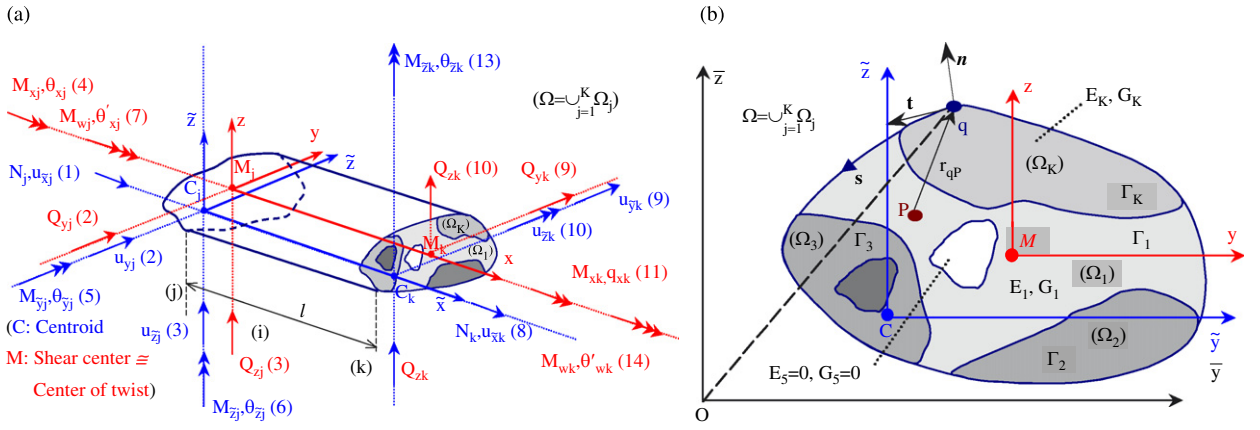

Fig. 1. Prismatic beam of an arbitrarily shaped composite cross section (a) and occupying the 2-D region Ω (b).

2.1. Torsional vibrations of composite bars

Defining as $E_1 C_M$ and $G_2 I_x$ the warping and torsional rigidities of the composite cross section, respectively, where

$$C_M = \sum_{j=1}^{K} \frac{E_j}{E_1} C_{Mj} = \sum_{j=1}^{K} \frac{E_j}{E_1} \int_{\Omega_j} (\varphi_M^P)_j^2 \, d\Omega_j, \tag{4a}$$

$$I_x = \sum_{j=1}^{K} \frac{G_j}{G_1} I_{xj} = \sum_{j=1}^{K} \frac{G_j}{G_1} \int_{\Omega_j} \left(y^2 + z^2 + y \left(\frac{\partial \varphi_M^P}{\partial z} \right)_j - z \left(\frac{\partial \varphi_M^P}{\partial y} \right)_j \right) d\Omega_j \tag{4b}$$

are its warping and torsion constants with respect to the modulus of elasticity and to the shear modulus, respectively, $\left(\varphi_M^P(y,z)\right)_j$ is the primary warping function with respect to the shear center M of the composite cross section of the bar and ignoring the additional inertia forces caused by the eccentricity between the centroid and center of twist, the angle of twist $\theta_x = \theta_x(x,t)$ of the bar subjected to the arbitrarily dynamic distributed twisting moment $m_x = m_x(x,t)$ is governed by the following initial boundary value problem [23,24]:

$$E_1 C_M \frac{\partial^4 \theta_x}{\partial x^4} - G_1 I_x \frac{\partial^2 \theta_x}{\partial x^2} - \rho_1 \left\{ C_M^\rho \frac{\partial^2}{\partial t^2} \left(\frac{\partial^2 \theta_x}{\partial x^2} \right) - I_M^\rho \frac{\partial^2 \theta_x}{\partial t^2} \right\} + c_t \frac{\partial \theta_x}{\partial t} = m_x \text{ inside the bar}, \tag{5}$$

$$c_{x1} \theta_x + c_{x2} M_x = c_{x3}, \tag{6a}$$

$$d_{x1} \theta_x' + d_{x2} M_w = d_{x3} \quad \text{at the bar ends } x = 0, l, \tag{6b}$$

$$\theta_x(x,0) = \bar{\theta}_x(x), \quad \dot{\theta}_x(x,0) = \dot{\bar{\theta}}_x(x), \tag{7a,b}$$

where $\dot{\theta}_x(x,t) = \partial \theta_x / \partial t$ is the first derivative of the angle of twist with respect to time; $\bar{\theta}_x(x)$, $\dot{\bar{\theta}}_x(x)$ are the initial angle of twist and the corresponding initial velocity of the points of the bar axis; c_t is the torsional damping constant per unit length; $\rho_1 C_M^\rho$ and $\rho_1 I_M^\rho$ is the mass moment of warping and torsional inertia, respectively, where C_M^ρ is the warping constant and I_M^ρ is the polar moment of inertia of the composite cross section with respect to the shear center (see Fig. 1) and to the mass density given as

$$C_M^\rho = \sum_{j=1}^{K} \frac{\rho_j}{\rho_1} C_{Mj}, \tag{8a}$$

$$I_M^{\rho} = \sum_{j=1}^{K} \frac{\rho_j}{\rho_1} \int_{\Omega_j} (y^2 + z^2)\, \mathrm{d}\Omega_j. \tag{8b}$$

Moreover, c_{xi}, $d_{xi} (i = 1, 2, 3)$ are functions specified at the boundary of the bar forming the most general linear torsional boundary conditions, including also the elastic support, while in Eqs. (6a) and (6b) $M_x = M_x(x, t)$ is the twisting moment and $M_w = M_w(x, t)$ is the warping moment at the boundary of the bar [25,26].

It is worth noting here that the reduction of Eqs. (4a), (4b) and (8a), (8b) using the modulus of elasticity E_1, the shear modulus G_1 and the mass density ρ_1 of the first material could be achieved using any other material of the composite cross section and modifying appropriately Eq. (5). Finally, the solution of the initial boundary value problem given from Eqs. (5), (6a), (6b) and (7a,b), which represents the dynamic nonuniform torsion problem of composite bars requires the evaluation of the warping and torsion constants C_{Mj} and I_{xj} of the j materials, $(j = 1, 2, \ldots, K)$, respectively, which is presented in Sapountzakis and Mokos [25].

2.2. Transverse vibrations of composite beams

Defining as $E_1 I_{\tilde{y}}$, $E_1 I_{\tilde{z}}$ the flexural rigidities of the composite cross section, where

$$I_{\tilde{y}} = \sum_{j=1}^{K} \frac{E_j}{E_1} \int_{\Omega_j} \tilde{z}^2\, \mathrm{d}\Omega_j, \quad I_{\tilde{z}} = \sum_{j=1}^{K} \frac{E_j}{E_1} \int_{\Omega_j} \tilde{y}^2\, \mathrm{d}\Omega_j \tag{9a,b}$$

are the bending moments of inertia of the composite cross section with respect to $\tilde{y}$, $\tilde{z}$ axes and to the modulus of elasticity and defining as $G_1 A_{\tilde{y}}$ and $G_1 A_{\tilde{z}}$ the shear rigidities of the Timoshenko's beam theory of the composite cross section, where

$$A_{\tilde{y}} = \kappa_{\tilde{y}} A_G = \frac{1}{a_{\tilde{y}}} A_G, \quad A_{\tilde{z}} = \kappa_{\tilde{z}} A_G = \frac{1}{a_{\tilde{z}}} A_G \tag{10a,b}$$

are the shear areas with respect to $\tilde{y}$, $\tilde{z}$ axes of the composite cross section, respectively, $\kappa_{\tilde{y}}$, $\kappa_{\tilde{z}}$ are the shear correction factors, $a_{\tilde{y}}$, $a_{\tilde{z}}$ are the shear deformation coefficients and A_G is the cross section area with respect to the shear modulus given as

$$A_G = \sum_{j=1}^{K} \frac{G_j}{G_1} \int_{\Omega_j} \mathrm{d}\Omega_j \tag{11}$$

the transverse displacements $u_{\tilde{z}} = u_{\tilde{z}}(\tilde{x}, t)$, $u_{\tilde{y}} = u_{\tilde{y}}(\tilde{x}, t)$ of the beam subjected to the arbitrarily distributed dynamic transverse loadings $p_{\tilde{z}} = p_{\tilde{z}}(\tilde{x}, t)$, $p_{\tilde{y}} = p_{\tilde{y}}(\tilde{x}, t)$ and to the arbitrarily distributed dynamic bending moments $m_{\tilde{y}} = m_{\tilde{y}}(\tilde{x}, t)$, $m_{\tilde{z}} = m_{\tilde{z}}(\tilde{x}, t)$, respectively (see Fig. 1) are governed by the following initial boundary value problems [27]:

(i) For $u_{\tilde{z}} = u_{\tilde{z}}(\tilde{x}, t)$

$$\begin{aligned} &\left\{ E_1 I_{\tilde{y}} \frac{\partial^4 u_{\tilde{z}}}{\partial \tilde{x}^4} + \rho_1 A^{\rho} \frac{\partial^2 u_{\tilde{z}}}{\partial t^2} \right\} - \left\{ \rho_1 I_{\tilde{y}}^{\rho} \frac{\partial^2}{\partial t^2} \left(\frac{\partial^2 u_{\tilde{z}}}{\partial \tilde{x}^2} \right) \right\} + \left\{ \frac{E_1 I_{\tilde{y}}}{G_1 A_{\tilde{z}}} \frac{\partial^2}{\partial \tilde{x}^2} \left(p_{\tilde{z}} - \rho_1 A^{\rho} \frac{\partial^2 u_{\tilde{z}}}{\partial t^2} \right) \right\} \\ &- \left\{ \frac{\rho_1 I_{\tilde{y}}^{\rho}}{G_1 A_{\tilde{z}}} \frac{\partial^2}{\partial t^2} \left(p_{\tilde{z}} - \rho_1 A^{\rho} \frac{\partial^2 u_{\tilde{z}}}{\partial t^2} \right) \right\} + c_{\tilde{z}} \frac{\partial u_{\tilde{z}}}{\partial t} = p_{\tilde{z}} + \frac{\partial m_{\tilde{y}}}{\partial \tilde{x}} \quad \text{inside the beam,} \end{aligned} \tag{12}$$

$$c_{\tilde{z}1} u_{\tilde{z}} + c_{\tilde{z}2} Q_{\tilde{z}} = c_{\tilde{z}3}, \tag{13a}$$

$$d_{\tilde{z}1} \theta_{\tilde{y}} + d_{\tilde{z}2} M_{\tilde{y}} = d_{\tilde{z}3} \quad \text{at the beam ends } \tilde{x} = 0, l, \tag{13b}$$

$$u_{\tilde{z}}(\tilde{x}, 0) = \bar{u}_{\tilde{z}}(\tilde{x}), \quad \dot{u}_{\tilde{z}}(\tilde{x}, 0) = \dot{\bar{u}}_{\tilde{z}}(\tilde{x}). \tag{14a,b}$$

(ii) For $u_{\tilde{y}} = u_{\tilde{y}}(\tilde{x}, t)$

$$\left\{E_1 I_{\tilde{z}} \frac{\partial^4 u_{\tilde{y}}}{\partial \tilde{x}^4} + \rho_1 A^{\rho} \frac{\partial^2 u_{\tilde{y}}}{\partial t^2}\right\} - \left\{\rho_1 I^{\rho}_{\tilde{z}} \frac{\partial^2}{\partial t^2}\left(\frac{\partial^2 u_{\tilde{y}}}{\partial \tilde{x}^2}\right)\right\} + \left\{\frac{E_1 I_{\tilde{z}}}{G_1 A_{\tilde{y}}} \frac{\partial^2}{\partial \tilde{x}^2}\left(p_{\tilde{y}} - \rho_1 A^{\rho} \frac{\partial^2 u_{\tilde{y}}}{\partial t^2}\right)\right\}$$
$$- \left\{\frac{\rho_1 I^{\rho}_{\tilde{z}}}{G_1 A_{\tilde{y}}} \frac{\partial^2}{\partial t^2}\left(p_{\tilde{y}} - \rho_1 A^{\rho} \frac{\partial^2 u_{\tilde{y}}}{\partial t^2}\right)\right\} + c_{\tilde{y}} \frac{\partial u_{\tilde{y}}}{\partial t} = p_{\tilde{y}} - \frac{\partial m_{\tilde{z}}}{\partial \tilde{x}} \quad \text{inside the beam,} \tag{15}$$

$$c_{\tilde{y}1} u_{\tilde{y}} + c_{\tilde{y}2} Q_{\tilde{y}} = c_{\tilde{y}3}, \tag{16a}$$

$$d_{\tilde{y}1} \theta_{\tilde{z}} + d_{\tilde{y}2} M_{\tilde{z}} = d_{\tilde{y}3} \quad \text{at the beam ends } \tilde{x} = 0, l, \tag{16b}$$

$$u_{\tilde{y}}(\tilde{x}, 0) = \bar{u}_{\tilde{y}}(\tilde{x}), \quad \dot{u}_{\tilde{y}}(\tilde{x}, 0) = \dot{\bar{u}}_{\tilde{y}}(\tilde{x}), \tag{17a,b}$$

where $\dot{u}_{\tilde{z}}(\tilde{x}, t) = \partial u_{\tilde{z}}/\partial t$, $\dot{u}_{\tilde{y}}(\tilde{x}, t) = \partial u_{\tilde{y}}/\partial t$ are the first derivatives of the transverse displacements $u_{\tilde{z}}$, $u_{\tilde{y}}$, respectively, with respect to time; $\bar{u}_{\tilde{z}}(\tilde{x})$, $\dot{\bar{u}}_{\tilde{z}}(\tilde{x})$ and $\bar{u}_{\tilde{y}}(\tilde{x})$, $\dot{\bar{u}}_{\tilde{y}}(\tilde{x})$ are the initial transverse displacements $u_{\tilde{z}}$, $u_{\tilde{y}}$ and the corresponding initial velocities of the points of the beam axis; $c_{\tilde{z}}$, $c_{\tilde{y}}$ are the flexural damping constants per unit length with respect to $\tilde{z}$, $\tilde{y}$ axes, respectively; $\rho_1 A^{\rho}$ is the mass per unit length and $\rho_1 I^{\rho}_{\tilde{y}}$, $\rho_1 I^{\rho}_{\tilde{z}}$ are the mass moments of rotatory inertia about the $\tilde{y}$, $\tilde{z}$ axes, respectively, where A^{ρ} is the cross section area and $I^{\rho}_{\tilde{y}}$, $I^{\rho}_{\tilde{z}}$ are bending moments of inertia of the composite cross section with respect to $\tilde{y}$, $\tilde{z}$ axes, respectively and to the mass density given as

$$A^{\rho} = \sum_{j=1}^{K} \frac{\rho_j}{\rho_1} \int_{\Omega_j} \mathrm{d}\Omega_j, \tag{18}$$

$$I^{\rho}_{\tilde{y}} = \sum_{j=1}^{K} \frac{\rho_j}{\rho_1} \int_{\Omega_j} \tilde{z}^2 \, \mathrm{d}\Omega_j, \tag{19a}$$

$$I^{\rho}_{\tilde{z}} = \sum_{j=1}^{K} \frac{\rho_j}{\rho_1} \int_{\Omega_j} \tilde{y}^2 \, \mathrm{d}\Omega_j. \tag{19b}$$

Moreover, $c_{\tilde{z}i}$, $d_{\tilde{z}i}$ and $c_{\tilde{y}i}$, $d_{\tilde{y}i} (i = 1, 2, 3)$ are functions specified at the boundary of the beam. The boundary conditions (13a), (13b) and (16a), (16b) are the most general linear flexural boundary conditions, including also the elastic support. In Eqs. (13a), (13b) and (16a), (16b) $Q_{\tilde{z}} = Q_{\tilde{z}}(\tilde{x}, t)$, $Q_{\tilde{y}} = Q_{\tilde{y}}(\tilde{x}, t)$ are the shear forces and $M_{\tilde{y}} = M_{\tilde{y}}(\tilde{x}, t)$, $M_{\tilde{z}} = M_{\tilde{z}}(\tilde{x}, t)$ are the bending moments at the boundary of the beam with respect to $\tilde{z}$, $\tilde{y}$ axes, respectively given as

$$Q_{\tilde{z}} = G_1 A_{\tilde{z}} \left(\frac{\partial u_{\tilde{z}}}{\partial \tilde{x}} + \theta_{\tilde{y}}\right), \quad Q_{\tilde{y}} = G_1 A_{\tilde{y}} \left(\frac{\partial u_{\tilde{y}}}{\partial \tilde{x}} - \theta_{\tilde{z}}\right), \tag{20a,b}$$

$$M_{\tilde{y}} = E_1 I_{\tilde{y}} \frac{\partial \theta_{\tilde{y}}}{\partial \tilde{x}}, \quad M_{\tilde{z}} = E_1 I_{\tilde{z}} \frac{\partial \theta_{\tilde{z}}}{\partial \tilde{x}}. \tag{21a,b}$$

It is worth here noting that the reduction of Eqs. (9), (11), (18) and (19) using the modulus of elasticity E_1, the shear modulus G_1 and the mass density ρ_1 of first material could be achieved using any other material of the composite cross section and modifying appropriately Eqs. (12), (15), (20) and (21).

The solution of the initial boundary value problems given from Eqs. (12), (13a), (13b), (14a,b) and (15), (16a), (16b), (17a,b), which represent the transverse vibrations of composite beams, presumes the evaluation of the shear deformation coefficients $a_{\tilde{y}}$, $a_{\tilde{z}}$, respectively, corresponding to the principal centroidal system of axes $C\tilde{y}\tilde{z}$. These coefficients are established equating the approximate formula of the shear strain energy per unit length [19] with the exact one given and are obtained as [27]

$$a_{\tilde{y}} = \frac{1}{\kappa_{\tilde{y}}} = \frac{A_G}{E_1 \Delta^2} \sum_{j=1}^{K} \int_{\Omega_j} E_j \Big((\nabla \Theta)_j - \mathbf{e}\Big) \cdot \Big((\nabla \Theta)_j - \mathbf{e}\Big) \, \mathrm{d}\Omega_j, \tag{22a}$$

$$a_{\tilde{z}} = \frac{1}{\kappa_{\tilde{z}}} = \frac{A_G}{E_1 \Delta^2} \sum_{j=1}^{K} \int_{\Omega_j} E_j \Big((\nabla \Phi)_j - \mathbf{d} \Big) \cdot \Big((\nabla \Phi)_j - \mathbf{d} \Big) \, d\Omega_j, \tag{22b}$$

where $(\tau_{\tilde{x}\tilde{z}})_j$, $(\tau_{\tilde{x}\tilde{y}})_j$ are the transverse (direct) shear stress components, $(\nabla)_j \equiv \mathbf{i}_{\tilde{y}}(\partial/\partial y)_j + \mathbf{i}_{\tilde{z}}(\partial/\partial z)_j$ is a symbolic vector with $\mathbf{i}_{\tilde{y}}$, $\mathbf{i}_{\tilde{z}}$ the unit vectors along $\tilde{y}$ and $\tilde{z}$ axes, respectively, Δ is given from

$$\Delta = 2(1+\nu) I_{\tilde{y}} I_{\tilde{z}}, \tag{23}$$

where ν is the Poisson's ratio of the cross section materials, which for the torsionless bending problem is assumed to be common, $\mathbf{e}$ and $\mathbf{d}$ are vectors defined as

$$\mathbf{e} = \left(\nu I_{\tilde{y}} \frac{\tilde{y}^2 - \tilde{z}^2}{2} \right) \mathbf{i}_{\tilde{y}} + \left(\nu I_{\tilde{y}} \tilde{y} \tilde{z} \right) \mathbf{i}_{\tilde{z}}, \tag{24a}$$

$$\mathbf{d} = \left(\nu I_{\tilde{z}} \tilde{y} \tilde{z} \right) \mathbf{i}_{\tilde{y}} + \left(\nu I_{\tilde{z}} \frac{\tilde{z}^2 - \tilde{y}^2}{2} \right) \mathbf{i}_{\tilde{z}} \tag{24b}$$

and $(\Theta(\tilde{y},\tilde{z}))_j$, $(\Phi(\tilde{y},\tilde{z}))_j$ are stress functions, which are evaluated from the solution of the following Neumann-type boundary value problems [28]

$$(\nabla^2 \Theta)_j = -2 I_{\tilde{y}} \tilde{y} \quad \text{in } \Omega_j (j = 1, 2, \ldots, K), , \tag{25a}$$

$$E_j \left(\frac{\partial \Theta}{\partial n} \right)_j - E_i \left(\frac{\partial \Theta}{\partial n} \right)_i = (E_j - E_i) \mathbf{n} \cdot \mathbf{e} \quad \text{on } \Gamma_j (j = 1, 2, \ldots, K), \tag{25b}$$

$$(\nabla^2 \Phi)_j = -2 I_{\tilde{z}} \tilde{z} \quad \text{in } \Omega_j (j = 1, 2, \ldots, K), \tag{26a}$$

$$E_j \left(\frac{\partial \Phi}{\partial n} \right)_j - E_i \left(\frac{\partial \Phi}{\partial n} \right)_i = (E_j - E_i) \mathbf{n} \cdot \mathbf{d} \quad \text{on } \Gamma_j (j = 1, 2, \ldots, K), \tag{26b}$$

where $\mathbf{n}$ is the outward normal vector to the boundary Γ_j ($E_i = 0$ at a free boundary). In the case of negligible shear deformations $a_{\tilde{z}} = a_{\tilde{y}} = 0$. It is worth here noting that in the most general case of a composite cross section with materials of different Poisson's ratios, the problem of torsionless bending becomes considerably more complicated, due to the fact that in this case the assumption of negligibly small stress components $(\sigma_{yy})_j$, $(\sigma_{zz})_j$ and $(\tau_{yz})_j$ is not correct [19]. However, having in mind that the values of the Poisson's ratios even for materials with significantly different elastic moduli are almost the same, it follows that the aforementioned assumption is realistic. Finally, the initial boundary value problem for the axial vibration of bars is presented in Humar [27].

3. Integral representations—numerical solution

3.1. For the angle of twist θ_x and the deflections $u_{\tilde{z}}$, $u_{\tilde{y}}$ and $u_{\tilde{x}}$

The numerical solution of the initial boundary value problems described by Eqs. (5), (6a), (6b), (7a,b), (12), (13a) (13b), (14a,b) (15), (16a), (16b), and (17a,b) is similar. Their solution is accomplished using BEM [22], as this is presented in Sapountzakis [29].

3.2. For the primary warping function $(\varphi_M^P)_j$

The evaluation of the primary warping function $(\varphi_M^P)_j$ is accomplished using BEM [22] as this is presented in in Sapountzakis and Mokos [25].

3.3. For the stress functions $(\Theta(y,z))_j$ and $(\Phi(y,z))_j$

The evaluation of the stress functions $(\Theta(y,z))_j$ and $(\Phi(y,z))_j$ is accomplished using BEM [22] as this is presented in Mokos and Sapountzakis [28].

4. Numerical examples

On the basis of the analytical and numerical procedures presented in the previous sections, a FORTRAN program has been written and representative examples have been studied to demonstrate the efficiency, wherever possible the accuracy and the range of applications of the developed method. In all the examples treated each cross section has been analyzed employing $N_{\mathrm{CS}} = 300$ constant boundary elements and $N_{\mathrm{Beam}} = 29$ constant elements along the axis of each beam, which are enough to ensure the convergence ($\varepsilon \leqslant 10^{-3}$) of the solution procedure.

Example 1. A cantilever slab and beam structure of composite cross section (Fig. 2a), of length $l = 5.00\,\mathrm{m}$, loaded at its free end by an eccentric concentrated load $P_{\tilde{z}}(\tilde{x},t) = P(t)\delta(\tilde{x}-l)$ (Fig. 2b), where $\delta(\tilde{x}-l)$ is the Dirac function, $P_o = 10\,\mathrm{kN}$, $t_1 = 0.02\,\mathrm{s}$, with material properties $E_{C35} = 3.35 \times 10^7\,\mathrm{kPa}$ (reference material), $E_{C20} = 2.90 \times 10^7\,\mathrm{kPa}$, $v = 0.16$, $\rho_{C35} = \rho_{C20} = 2500\,\mathrm{kg/m^3}$, damping ratio $\xi = 0$, and cross section properties $A_G = A_E = 0.76628\,\mathrm{m^2}$, $A^{\rho} = 0.82\,\mathrm{m^2}$, $\kappa_{\tilde{z}} = 3.04033\mathrm{E}-01$, $I_{\tilde{y}} == 9.83021\mathrm{E}-02\,\mathrm{m^4}$, $I^{\rho}_{\tilde{y}} = 10.2324\mathrm{E}-02\,\mathrm{m^4}$, $I^{\rho}_M = 2.68615\mathrm{E}-01\,\mathrm{m^4}$, $I_x = 2.22768\mathrm{E}{-}02\,\mathrm{m^4}$, $C_M = 2.22217\mathrm{E}{-}03\,\mathrm{m^6}$, $C^{\rho}_M = 2.32248\mathrm{E}-03\,\mathrm{m^6}$, $e_M = 1.29767\mathrm{E}{-}01\,\mathrm{m}$ (between the centroid C with respect to mass density and the center of twist M with respect to modulus of elasticity of the composite cross section) has been studied. In Fig. 3 the boundary distribution of the primary warping function φ^P_M of the composite cross section of the slab and beam structure is presented. From this figure it follows that torsional warping is not constant along the thickness of the cross section walls as it is assumed in Thin Tube Theory for thin-walled beams. In Table 1 the first five eigenfrequencies of the axially free vibrating structure are presented as compared wherever possible with those obtained from an analytic solution employing a continuous system [27] and from a 3-D finite-element solution [30] using 600 and 4000 eight-noded hexahedral solid elements, respectively. From this table the accuracy of the results of the proposed method is remarkable. Moreover, in Fig. 4 the first five modeshapes obtained from the proposed solution of the axially free vibrating beam are presented. In Table 2 the first five eigenfrequencies of the torsionally free vibrating beam are presented as compared with those obtained ignoring torsional warping

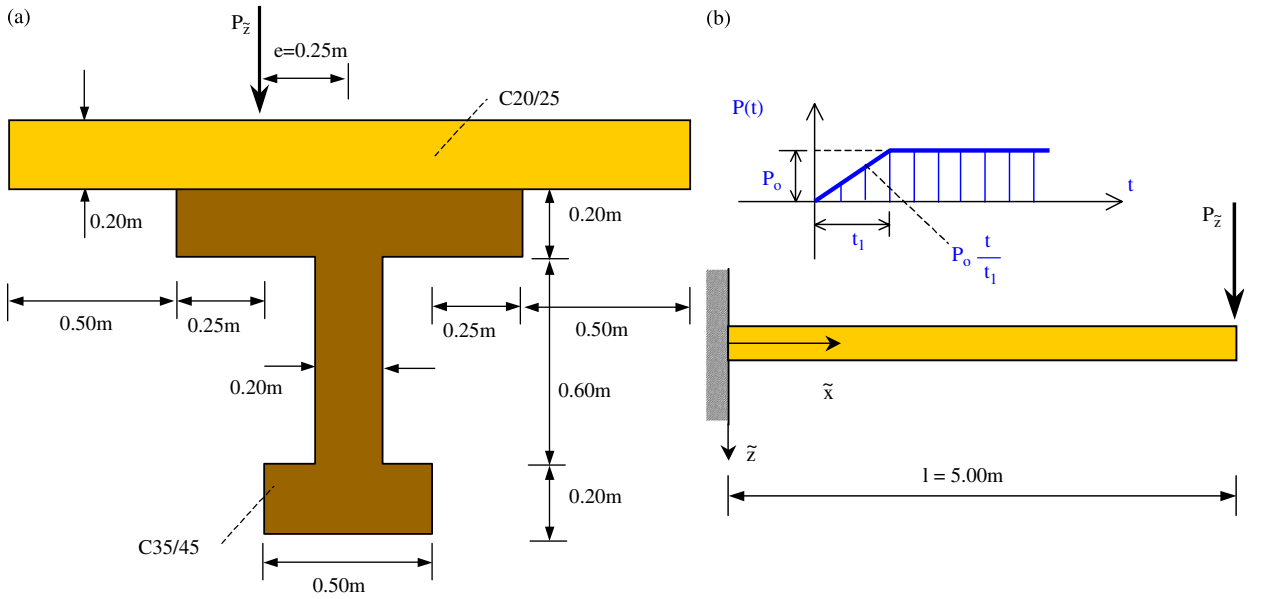

Fig. 2. Cantilever slab and beam structure of Example 1 of composite cross section (a), loaded at its free end by an eccentric concentrated dynamic load $P_{\tilde{z}}(t)$ (b).

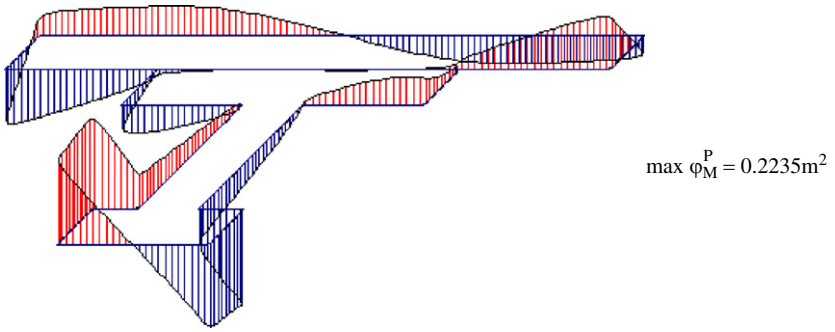

Fig. 3. Distribution of the primary warping function φ_M^P of the composite cross section of the cantilever slab and beam structure of Example 1.

Table 1
Eigenfrequencies ω_i (rad/s) for the axial free vibration of the cantilever slab and beam composite structure of Example 1

ω_i	BEM (CPU: 2 s)	Continuous systems [27]	3-D FEM [30] (600 Solid FE) (CPU: 24 s)	3-D FEM [30] (4000 Solid FE) (CPU: 35 s)
1	1111.659	1111.141	1116.189	1111.927
2	3333.878	3333.422	3419.023	3413.038
3	5552.808	5555.703	5773.001	5703.005
4	7766.258	7777.985	7994.1113	7914.1331
5	9972.044	10000.266	10079.234	10018.119

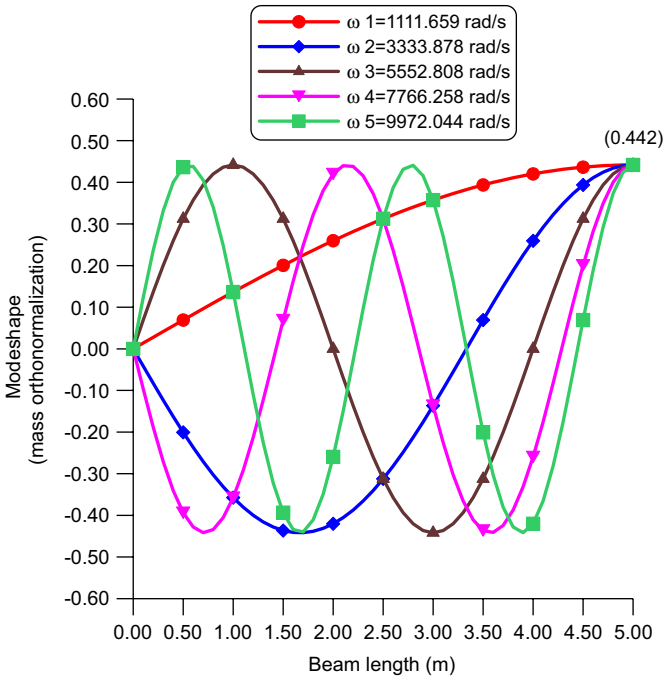

Fig. 4. First five modeshapes of the axially free vibrating cantilever slab and beam composite structure of Example 1.

behavior (12 dof of the classical 3-D frame element), with those obtained taking into account or ignoring warping inertia (with 14 dof) and wherever possible with those obtained from a 3-D finite-element solution [30] using 600 and 4000 eight-noded hexahedral solid elements, respectively. From this table, the accuracy of

Table 2
Eigenfrequencies ω_i (rad/s) of the torsionally free vibrating cantilever slab and beam composite structure of Example 1

ω_i	BEM (CPU: 16 s)			3-D FEM [30] (600 Solid FE) (CPU: 29 s)	3-D FEM [30] (4000 Solid FE) (CPU: 38 s)
	12×12 member stiffness matrix	14×14 member stiffness matrix			
	With torsional inertia	With torsional inertia	With torsional and warping inertia		
1	217.426	242.6208	242.5074	244.124	242.623
2	652.124	775.3973	772.1076	770.234	760.101
3	1086.361	1439.223	1422.253	1335.254	1385.232
4	1519.827	2293.520	2241.344	2245.157	2237.593
5	1952.216	3374.459	3251.226	3315.172	3305.263

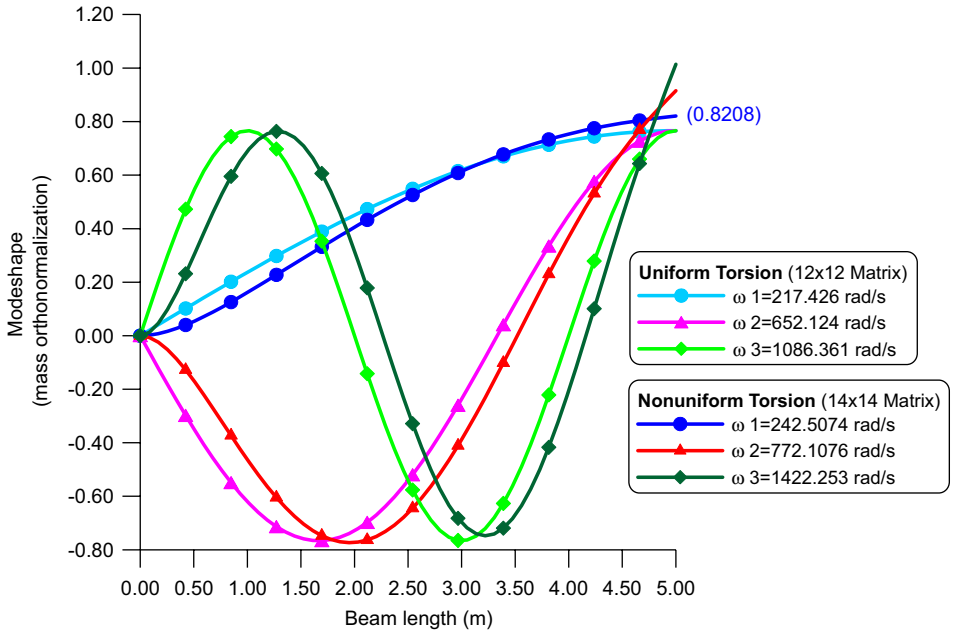

Fig. 5. First three modeshapes of the torsionally free vibrating cantilever slab and beam composite structure of Example 1.

the results of the proposed method is once more verified, the ignorance of the torsional warping behavior proves to be prohibitive, while the discrepancy of the results arising from the ignorance of the warping inertia especially in higher eigenfrequencies is noteworthy. Moreover, in Fig. 5 the first three modeshapes obtained from the proposed solution employing either the 12 dof classical 3-D frame element or the 14 dof one taking into account the warping inertia are presented. With regard to the computed mode shapes, though the nodal patterns of corresponding modeshapes remain the same, the normalized modal angles of twist are significantly different. In Table 3 the first five eigenfrequencies of the transversely free vibrating beam are presented as compared with those obtained taking into account or ignoring shear deformation, with those obtained taking into account or ignoring rotary inertia and wherever possible with those obtained from a 3-D finite-element solution [30] using 600 and 4000 eight-noded hexahedral solid elements, respectively. From this table, the accuracy of the results of the proposed method (comparison between the results of the 3-D FEM solution and those obtained taking into account both shear deformation and rotary inertia) is once more verified, the ignorance of the shear deformation proves to be prohibitive, while the discrepancy of the results arising from the ignorance of the rotary inertia especially in higher eigenfrequencies is remarkable. Moreover, in Fig. 6 the

Table 3
Eigenfrequencies ω_i (rad/s) of the transversely free vibrating in z direction cantilever slab and beam composite structure of Example 1

ω_i	BEM (CPU: 14 s)				3-D FEM [30] (600 Solid FE) (CPU: 26 s)	3-D FEM [30] (4000 Solid FE) (CPU: 37 s)
	Without shear deformation		With shear deformation			
	With transverse inertia	With transverse and rotary inertia	With transverse inertia	With transverse and rotary inertia		
1	178.229	176.195	163.798	162.961	165.746	163.147
2	1116.583	1035.722	742.984	739.072	747.594	745.631
3	3125.550	2657.422	1601.622	1591.092	1599.841	1597.968
4	6122.996	4690.369	2465.149	2456.699	2877.128	2459.699
5	10118.64	6956.457	3326.177	3300.071	3515.869	3308.085

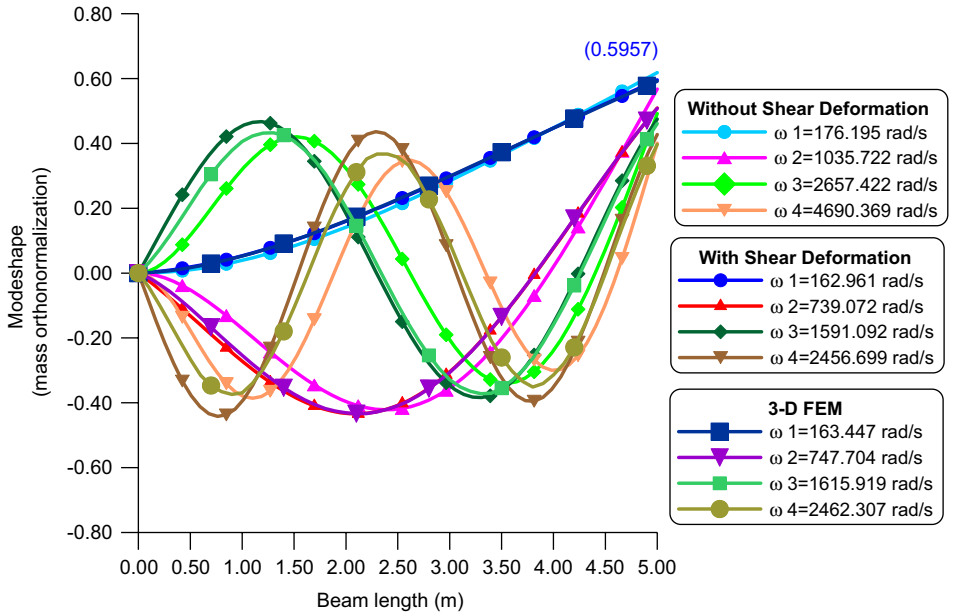

Fig. 6. First four modeshapes of the transversely free vibrating in z direction cantilever slab and beam composite structure of Example 1.

first four modeshapes obtained from the proposed solution taking into account or ignoring shear deformation and including rotary inertia are presented. With regard to the computed mode shapes, though the nodal patterns of corresponding modeshapes remain the same, the normalized modal deflections are significantly different.

It is worth here noting the major merit of the aforementioned accuracy of the proposed method compared with the 3-D FEM solution using solid elements, arising from the disadvantages of the latter due to the difficulties of

- support modelling;
- discretizing a complex structure despite the existing element generators;
- discretizing a structure including thin-walled members (shear-locking, membrane-locking [31]);
- increased number of dof leading to severe or unrealistic computational time especially for structures consisting of many elements;
- reduced oversight of the 3-D FEM solution compared with that of the beam-like structures employing stress resultants.

Table 4
Angle of twist $\max \theta_x^{\mathrm{dyn}}$(rad) and dynamic magnification factor at the fifths of the beam length $l(m)$, of the cantilever slab and beam composite structure of Example 1

l	With torsional inertia			With torsional and warping inertia		
	$\max \theta_x^{\mathrm{dyn}} \times 10^5$	$\theta_x^{\mathrm{static}} \times 10^5$	D_θ	$\max \theta_x^{\mathrm{dyn}} \times 10^5$	$\theta_x^{\mathrm{static}} \times 10^5$	D_θ
12×12 member stiffness matrix						
1	1.154778	0.790349	1.461098	–	–	–
2	2.300025	1.580699	1.455068	–	–	–
3	3.374221	2.371049	1.423092	–	–	–
4	4.329542	3.161398	1.369503	–	–	–
5	5.103968	3.885885	1.313464	–	–	–
14×14 member stiffness matrix						
1	0.653125	0.461627	1.414832	0.650943	0.461627	1.410105
2	1.660572	1.212281	1.369791	1.658610	1.212281	1.368173
3	2.632601	1.997837	1.317725	2.632743	1.997837	1.317797
4	3.556093	2.787605	1.275681	3.558246	2.787605	1.276453
5	4.372269	3.512015	1.244946	4.371209	3.512015	1.244644

While the use of shell elements cannot give accurate results since the warping of the walls of a cross section cannot be taken into account (midline model).

Moreover, noting Tables 1–3 it follows that for the analysis of this example with the presented numerical procedures the maximum CPU time needed at a Personal Computer Intel(R) 2.00 GHz is less than 16 s, while the corresponding one using 600 and 4000 eight-noded hexahedral solid elements is less than 29 and 38 s, respectively. This remark demonstrates the convergence and stability of the proposed method and that the CPU times of the presented numerical procedures are competitive with those of a standard 3-D FEM approach.

According to the forced vibrations case, in Tables 4 and 5 the maximum values of the angle of twist $\max \theta_x^{\mathrm{dyn}}$ and the deflection in z direction $\max u_{\bar{z}}^{\mathrm{dyn}}$ are shown together with the corresponding static ones $\theta_x^{\mathrm{static}}$, $u_{\bar{z}}^{\mathrm{static}}$ for the calculation of the dynamic magnification factor $D = \max |R(t)|$, $R_\theta(t) = \theta_x^{\mathrm{dyn}}/\theta_x^{\mathrm{static}}$, $R_u(t) = u_{\bar{z}}^{\mathrm{dyn}}/u_{\bar{z}}^{\mathrm{static}}$ taking into account or ignoring torsional warping behavior, warping inertia and shear deformation, rotary inertia, respectively. Moreover, in Fig. 7 the time history of the angle of twist θ_x at the free end of the cantilever beam is presented as compared with this obtained ignoring torsional warping behavior, while in Fig. 8 the time history of the deflection in z direction $u_{\bar{z}}$ at the same point is presented as compared with this obtained ignoring shear deformation effect. The conclusions drawn for the free vibrations case are also verified for the forced vibrations one.

Example 2. A curved clamped beam of length $l = 80.00$ m, of composite cross section consisting of a concrete C30/37 ($E_C = 3.2 \times 10^7$ kPa, $\rho_C = 2500\,\mathrm{kg/m^3}$) part (reference material) stiffened by a steel Fe510 ($E_S = 2.1 \times 10^8$ kPa, $\rho_S = 7850\,\mathrm{kg/m^3}$) one, forming a box shaped closed cross section, with uniform Poisson's $\nu = 0.20$ and damping $\xi = 0.04$ ratios and cross section properties $A_G = A_E = 6.01600\,\mathrm{m^2}$, $A^\rho = 4.25273\,\mathrm{m^2}$, $\kappa_{\bar{z}} = 0.20945$, $I_{\bar{y}} = 3.73790\,\mathrm{m^4}$, $I_{\bar{y}}^\rho = 2.35666\,\mathrm{m^4}$, $I_M^\rho = 20.02965\,\mathrm{m^4}$, $I_x = 6.07669\,\mathrm{m^4}$, $C_M = 1.50533\,\mathrm{m^6}$, $C_M^\rho = 0.53237\,\mathrm{m^6}$, $e_M = 0.47226$ m (between the centroid C with respect to mass density and the center of twist M with respect to modulus of elasticity of the composite cross section) has been studied (Fig. 9). In Table 6 the first five eigenperiods of the free vibrating discretized structural model (Fig. 10) of the curved beam are presented as compared with those obtained taking into account or ignoring torsional warping behavior (14 instead of 12 dof), shear deformation and rotary, torsional and warping inertia. As it is easily verified from this table due to the closed form of the beam cross section torsional warping behavior can be neglected. Finally, the presented curved beam has been examined in forced vibrations induced by a centrally applied (point C) concentrated dynamic load $P_{\bar{z}}(\bar{x}, t) = P_o H(t)\delta(\bar{x} - l/2, \bar{y} - h)$ (Fig. 9a and b), where $\delta(\bar{x} - l/2, \bar{y} - h)$ is the Dirac function in two dimensions, $H(t)$ is the Heaviside function, $P_o = 100$ kN, $t_1 = 0.5$ s. In Fig. 11 the time history of the deflection in z direction $u_{\bar{z}}$ at section C (Fig. 9) is presented as compared with this obtained ignoring shear deformation effect.

Table 5
Deflection $\max u_{\bar{z}}^{\mathrm{dyn}}(m)$ in z direction and dynamic magnification factor at the fifths of the beam length $l(m)$, of the cantilever composite structure of Example 1

l	With transverse inertia			With transverse and rotary inertia		
	$\max u_{\bar{z}}^{\mathrm{dyn}} \times 10^5$	$u_{\bar{z}}^{\mathrm{static}} \times 10^5$	D_u	$\max u_{\bar{z}}^{\mathrm{dyn}} \times 10^5$	$u_{\bar{z}}^{\mathrm{static}} \times 10^5$	D_u
Without shear deformation						
1	1.184323	0.731883	1.618186	1.188926	0.731883	1.624477
2	4.328752	2.714620	1.594607	4.348420	2.714620	1.601852
3	8.837667	5.628844	1.570068	8.886009	5.628844	1.578656
4	14.17125	9.155189	1.547893	14.25474	9.155189	1.557012
5	19.41739	12.65264	1.534651	19.53355	12.65264	1.543832
With shear deformation						
1	1.826575	1.034173	1.766218	1.824482	1.034173	1.764194
2	5.628834	3.319200	1.695841	5.634514	3.319200	1.697552
3	10.75720	6.535714	1.645911	10.79082	6.535714	1.651054
4	16.65847	10.36435	1.607285	16.72168	10.36435	1.613385
5	22.36327	14.13890	1.581684	22.45749	14.13890	1.588348

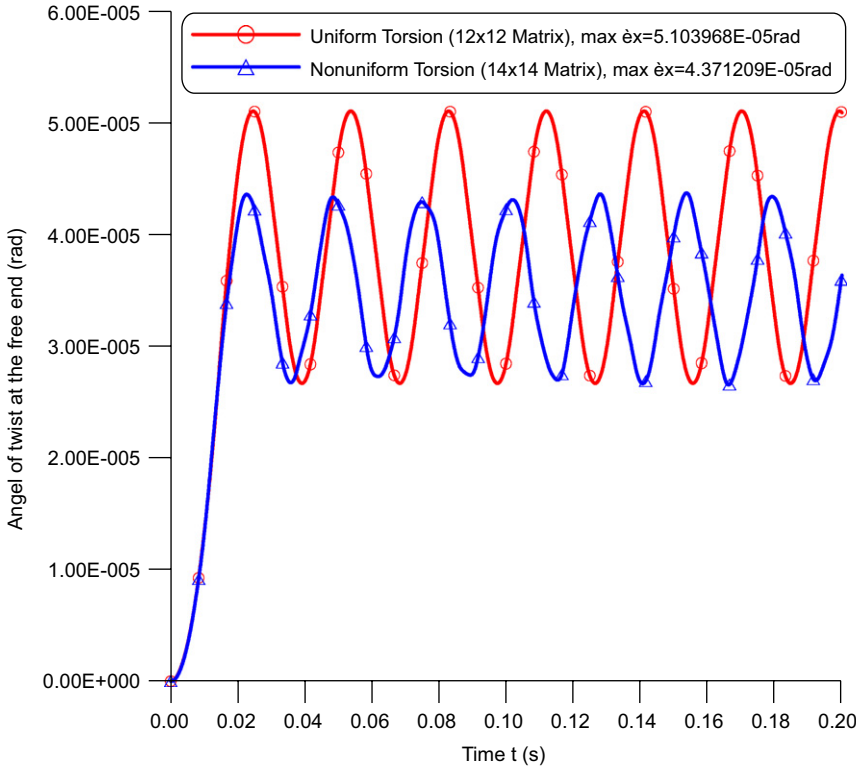

Fig. 7. Time history of the angle of twist θ_x at the free end of the cantilever slab and beam composite structure of Example 1.

5. Concluding remarks

In this paper, the dynamic analysis of 3-D composite beam elements restrained at their edges by the most general linear torsional, transverse or longitudinal boundary conditions and subjected in arbitrarily

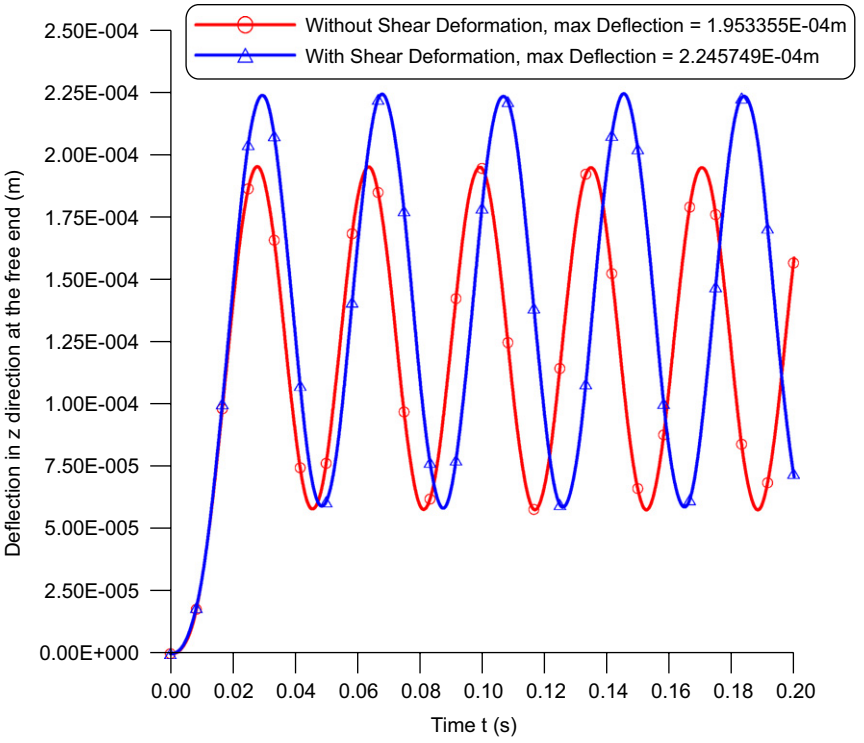

Fig. 8. Time history of the deflection in z direction $u_{\bar{z}}$ at the free end of the cantilever composite structure of Example 1.

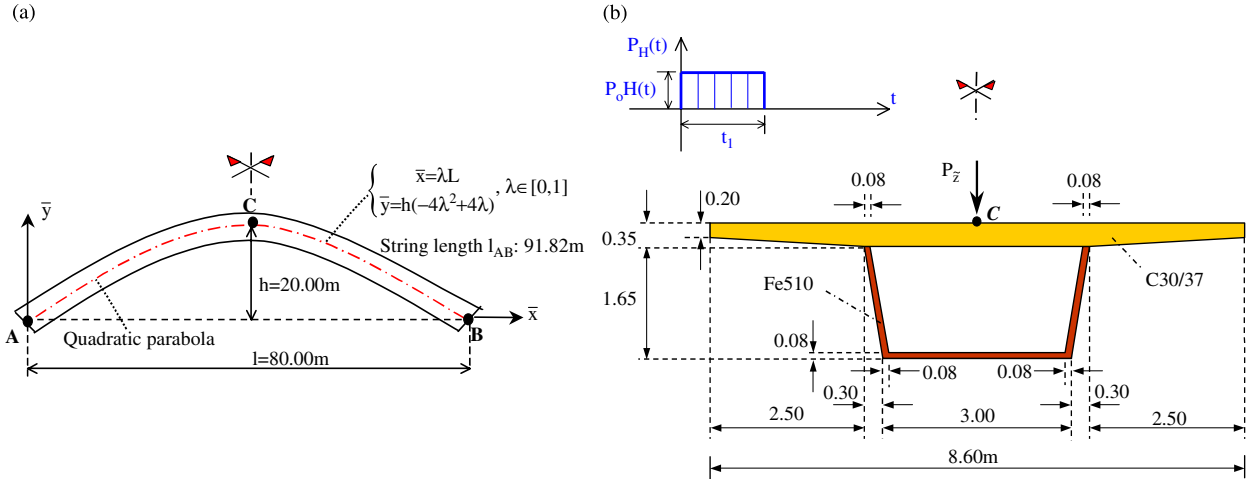

Fig. 9. Plan view (a) and composite cross section and (b) of the curved clamped beam of Example 2.

distributed dynamic twisting, bending, transverse or longitudinal loading is presented. For the solution of the problem at hand, a boundary element method is developed for the construction of the 14×14 stiffness matrix and the nodal load vector, of a member of an arbitrarily shaped composite cross section, taking into account both torsional warping and shear deformation effects, which together with the corresponding mass and damping matrices lead to the formulation of the equation of motion. The composite member consists of materials in contact each of which can surround a finite number of inclusions. All the cross section materials is

Table 6
Eigenperiods T_i of the curved clamped composite beam of Example 2

Eigenperiods T_i(s)	14×14 member stiffness matrix		12×12 member stiffness matrix	
	Including shear deformation	Ignoring shear deformation	Including shear deformation	Ignoring shear deformation
Including transverse, rotary, torsional and warping inertia			*Including transverse, rotary, torsional inertia and ignoring warping inertia*	
1	8.590900E−01	8.455086E−01	8.592216E−01	8.456429E−01
2	2.917596E−01	2.805310E−01	2.918888E−01	2.806597E−01
3	1.502124E−01	1.406928E−01	1.502664E−01	1.407642E−01
4	1.127833E−01	1.117127E−01	1.139600E−01	1.128813E−01
5	9.201591E−02	8.344578E−02	9.204184E−02	8.347931E−02
Including transverse inertia and ignoring rotary, torsional and warping inertia				
1	8.550508E−01	8.412664E−01	8.551674E−01	8.413849E−01
2	2.897008E−01	2.782027E−01	2.897982E−01	2.782970E−01
3	1.469535E−01	1.368381E−01	1.469760E−01	1.368620E−01
4	9.028992E−02	8.115724E−02	9.030397E−02	8.117244E−02
5	6.228844E−02	5.380419E−02	6.229755E−02	5.381445E−02

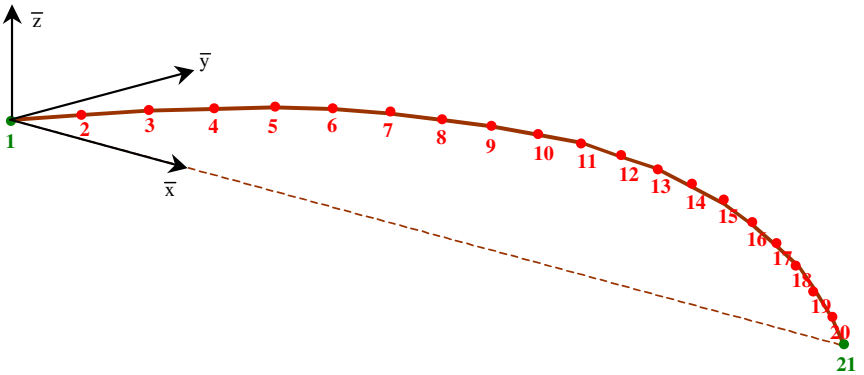

Fig. 10. Discretized structural model of the curved clamped beam of Example 2.

assumed to have the same Poisson's ratio. To account for shear deformations, the concept of shear deformation coefficients is used, defining these factors using a strain energy approach. Both free and forced transverse, longitudinal or torsional vibrations are considered, taking also into account effects of transverse, longitudinal, rotatory, torsional and warping inertia and damping resistance. The main conclusions that can be drawn from this investigation are:

(a) The numerical technique presented in this investigation is well suited for computer-aided analysis.
(b) The accuracy of the obtained results compared with those obtained from a 3-D FEM solution is remarkable. Having in mind both the disadvantages of the 3-D FEM solution using solid elements (difficulties in support modelling, in discretizing a complex structure, in discretizing a structure including thin-walled members (shear-locking, membrane-locking), in the increased number of dof leading to severe or unrealistic computational time, in the reduced oversight of the 3-D FEM solution compared with that of the beam-like structures employing stress resultants) and the fact that the use of shell elements cannot give accurate results since the warping of the walls of a cross section cannot be taken into account (midline model), the importance of the proposed method becomes more evident.
(c) Torsional warping is not constant along the thickness of the cross section walls as it is assumed in Thin Tube Theory for thin-walled beams.

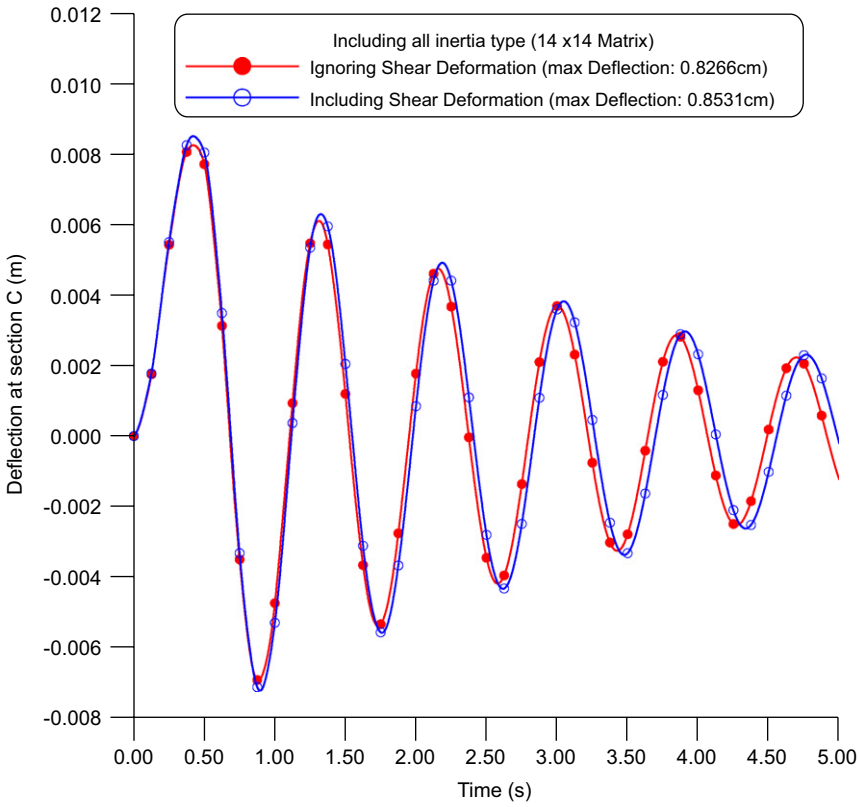

Fig. 11. Deflection response at section C of the curved clamped beam of Example 2.

(d) The discrepancy of the results arising from the ignorance of the torsional warping dof at the ends of a member necessitate the utilization of the 14×14 member stiffness matrix, especially for beams with open form cross section.
(e) The considerable influence of the shear deformation effect in the deflection and the internal stress resultants is pointed out.
(f) The discrepancy of the results arising from the ignorance of either the warping or the rotary inertia especially in higher eigenfrequencies is noteworthy.
(g) The advantages of a box shaped closed cross section beam subjected in torsional loading compared with that of an open one are easily verified.
(h) The developed procedure retains the advantages of a BEM solution over a pure domain discretization method since it requires only boundary discretization.

Acknowledgements

Financial support provided by the "HRAKLEITOS Research Fellowships with Priority to Basic Research", an EU funded project in the special managing authority of the Operational Program in Education and Initial Vocational Training. The Project "HRAKLEITOS" is co-funded by the European Social Fund (75%) and National Resources (25%).

References

[1] ANSYS, Engineering Solution, Version 7.0, USA, 2002.
[2] SOFiSTiK AG, Finite Elemente & CAD Software für den Ingenieurbau, Germany, 2006.

[3] J. Murin, V. Kutis, 3D-beam element with continuous variation of the cross-sectional area, *Computers and Structures* 80 (2002) 329–338.
[4] R.J. Reilly, Stiffness analysis of grid including warping, *Journal of Structural Division, ASCE* 7 (1972) 1511–1523.
[5] R.S. Barsoum, R.H. Gallagher, Finite element analysis of torsional-flexural stability problems, *International Journal for Numerical Methods in Engineering* 2 (1970) 335–352.
[6] P. Waldron, Elastic analysis of curved thin-walled girders including the effect of warping restraint, *Engineering Structures* 7 (1985) 93–104.
[7] P. Waldron, Stiffness analysis of thin-walled girders, *Journal of Structural Division, ASCE* 6 (1986) 1366–1384.
[8] Y. Yang, W. McGuire, A procedure for analyzing space frames with partial warping restraint, *International Journal for Numerical Methods in Engineering* 20 (1984) 1377–1398.
[9] M.Z. Ahmed, F.E. Weisgerber, Torsion constant for matrix analysis of structures including warping effect, *International Journal of Solids and Structures* 33 (1996) 361–374.
[10] M. Karama, K.S. Afaq, S. Mistou, Mechanical behavior of laminated composite beam by the new multi-layered laminated composite structures model with transverse shear stress continuity, *International Journal of Solids and Structures* 40 (6) (2003) 1525–1546.
[11] M. Touratier, A refined theory of laminated shallow shells, *International Journal of Solids and Structures* 29 (11) (1992) 1401–1415.
[12] J.N. Reddy, On refined computational models of composite laminates, *International Journal for Numerical Methods in Engineering* 27 (1989) 361–382.
[13] M. Mitra, S. Gopalakrishnan, M.S. Bhat, A new super convergent thin walled composite beam element for analysis of box beam structures, *International Journal of Solids and Structures* 41 (2004) 1491–1518.
[14] C. Bach, R. Baumann, *Elastizität und Festigkeit*, ninth ed., Springer, Berlin, 1924.
[15] D. Stojek, Zur Schubverformung im Biegebalken, *Zeitschrift für Angewandte Mathematik und Mechanik* 44 (1964) 393–396.
[16] S.P. Timoshenko, J.N. Goodier, *Theory of Elasticity*, third ed., McGraw-Hill, New York, 1984.
[17] G.R. Cowper, The shear coefficient in Timoshenko's Beam Theory, *Journal of Applied Mechanics, ASME* 33 (2) (1966) 335–340.
[18] U. Schramm, V. Rubenchik, W.D. Pilkey, Beam stiffness matrix based on the elasticity equations, *International Journal for Numerical Methods in Engineering* 40 (1997) 211–232.
[19] W.D. Pilkey, *Analysis and Design of Elastic Beams—Computational Methods*, Wiley, New York, 2002.
[20] N.G. Stephen, Timoshenko's shear coefficient from a beam subjected to gravity loading, *Journal of Applied Mechanics, ASME* 47 (1980) 121–127.
[21] J.R. Hutchinson, Shear coefficients for Timoshenko beam theory, *Journal of Applied Mechanics, ASME* 68 (2001) 87–92.
[22] J.T. Katsikadelis, *Boundary Elements: Theory and Applications*, Elsevier, Amsterdam, London, 2002.
[23] M. Tanaka, A.N. Bercin, Finite element modelling of the coupled bending and torsional free vibration of uniform beams with an arbitrary cross-section, *Applied Mathematical Modelling* 21 (1997) 339–344.
[24] A. Prokić, On triply coupled vibrations of thin-walled beams with arbitrary cross-section, *Journal of Sound and Vibration* 279 (2005) 723–737.
[25] E.J. Sapountzakis, V.G. Mokos, Warping shear stresses in nonuniform torsion of composite bars by BEM, *Computer Methods in Applied Mechanics and Engineering* 192 (2003) 4337–4353.
[26] E.J. Sapountzakis, Torsional vibrations of composite bars of variable cross section by BEM, *Computer Methods in Applied Mechanics and Engineering* 194 (2005) 2127–2145.
[27] J.L. Humar, *Dynamics of Structures*, second ed., A.A. Balkema Publishers, Lisse, Abingdon, Exton (PA), Tokyo, 2002.
[28] V.G. Mokos, E.J. Sapountzakis, A BEM solution to transverse shear loading of composite beams, *International Journal of Solids and Structures* 42 (2005) 3261–3287.
[29] E.J. Sapountzakis, Torsional vibrations of composite bars by BEM, *Composite Structures* 70 (2005) 229–239.
[30] MSC/NASTRAN for Windows, Finite element modeling and postprocessing system, Help System Index, Version 4.0, USA, 1999.
[31] K. Knothe, H. Wessels, *Finite Elemente, 2. Auflage*, Springer, Berlin, New York, 1992 (in German).